Structure and Dynamics of Self-Assembling Aluminum Didodecyl Phosphate Organogels

Miles G. Page[†] and Gregory G. Warr*

School of Chemistry, The University of Sydney, NSW 2006, Australia

Received: July 4, 2004; In Final Form: August 19, 2004

A self-assembled organogel of aluminum isopropoxide and didodecyl phosphate surfactant in decane is studied as a function of the ratio of aluminum:surfactant. The rheology and structure is shown to depend sensitively on this ratio. Small angle neutron scattering shows the aggregates to be locally cylindrical and molecularly thin at all compositions studied. In the presence of excess surfactant, the system displays Maxwellian rheology and behavior reminiscent of transient, entangled networks of wormlike micelles. A large transition in the relaxation time of the system occurs over a narrow composition range near stoichiometric equivalence (aluminum:surfactant = 1:3), indicating the formation of a connected network with physical gel behavior. At a large excess of aluminum this results in a phase separation into gel and nonviscoelastic liquid. The formation of the gel network and subsequent phase separation are rationalized in terms of localized branch points formed in the aggregates by the excess of aluminum isopropoxide.

Introduction

Viscoelastic organic solutions and organogels formed by the self-assembly of low molecular weight solute species are of interest as substitutes for conventional polymers in a wide range of applications.[1] Small solute molecules frequently have solubility and kinetic advantages over polymer solutions; however, much less is known about self-assembly in nonaqueous, nonpolar solvents than in water.[2−4]

Known mechanisms of self-assembly in nonpolar solvents include networks of hydrogen-bonded fatty acid or cholesterol headgroups,[5,6] reverse microemulsions such as the extensively studied lecithin/water/oil systems,[7] or the stacking of organometallic compounds through internuclear complexation.[8,9] The mechanism by which these and other small organogelators form extended aggregates and gel the organic phase has recently been reviewed.[1]

Aluminum dialkyl phosphates are an example of low molecular weight organogelators, and have been a material of choice in hydraulic fracturing fluids since their development in this field in the 1970s.[10] To date there has been very little investigation of their structure and dynamics, except for Fukasawa et al.,[8] who studied the behavior of aluminum dihexadecyl phosphate salt in hexadecane. On the basis of X-ray diffraction and differential scanning calorimetry measurements, they concluded that the structure was of long cylindrical (rodlike) aggregates, with an aluminum core surrounded by dialkyl phosphate. On the basis of prior studies into metal alkyl phosphinates,[11,12] the stability was proposed to result from the dialkyl phosphate forming bridges between neighboring aluminum ions. The structure is shown schematically in Figure 1.

In this work an in situ technique[13] is used, in which aluminum isopropoxide is added to a solution of didodecylphosphoric acid in oil

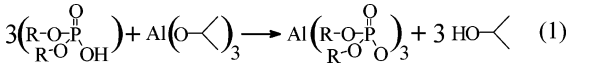

(1)

where R = $C_{12}H_{25}$ for didodecyl phosphate.

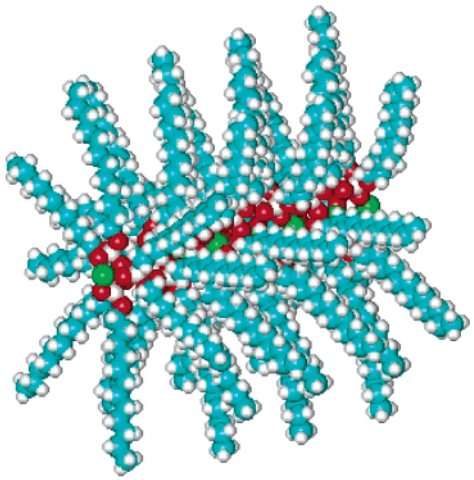

Figure 1. Schematic of the proposed structure of aluminum dihexadecyl phosphate, as determined from X-ray diffraction studies.[8] Color key: green, aluminum; red, oxygen, phosphorus; blue, carbon; white, hydrogen.

To our knowledge, there has been only one previous study of aluminum alkyl phosphate gels employing this technique outside the patent literature.[14]

In situ preparation allows the properties of the organogel to be controlled by varying the ratio of aluminum isopropoxide to didodecyl phosphate ("Al:P") in the system away from that of the neutral salt (1:3). We find that this simple change in composition has a profound effect on the rheology of the system. We combine rheological characterization with small angle neutron scattering (SANS) at various Al:P ratios and gellant concentrations to determine the underlying self-assembly structure responsible for the observed mechanical properties.

Materials and Methods

The surfactant didodecyl phosphoric acid was kindly provided by Dr. Robert Reierson from Rhodia Inc, twice recrystallized, and was used as received. Aluminum isopropoxide (99+%) was purchased from Sigma-Aldrich. The various organogels were prepared in decane (99+%) for rheological studies, or perdeuterated decane (99 atom %) for SANS, also from Sigma-Aldrich.

* Author to whom correspondence should be sent. E-mail g.warr@chem.usyd.edu.au.

[†] Current address: Max Planck Institute for Colloids and Interfaces, Am Mühlenberg 1, 14476 Golm, Germany.

10.1021/jp0470602 CCC: $27.50
Published on Web 10/05/2004

Gels were prepared under nitrogen. The acid of didodecyl phosphate was dissolved in decane at ~40 °C at the desired concentration (by mass). The required molar amount of aluminum isopropoxide was then added also by mass with continuous stirring. Gelation generally occurred immediately upon addition of the aluminum; however, the mixture was then covered, heated to ~150 °C, and stirred for up to several hours to allow equilibration.

Rheological measurements were performed at 25 ± 0.1 °C on a Reologica Stresstech controlled stress rheometer in either cone-and-plate or parallel-plate geometry. Linear viscoelasticity at the selected strain amplitudes was verified by strain sweep experiments. Typically linear viscoelasticity was found for amplitudes of ≤0.2.

In most cases the rheological data are well described by a single relaxation time Maxwell model. The equations describing the storage and loss moduli, G' and G'' in this case, are given by[15]

$$G'(\omega) = \frac{G_0\omega^2\tau^2}{1+\omega^2\tau^2} \tag{2}$$

$$G''(\omega) = \frac{G_0\omega\tau}{1+\omega^2\tau^2} \tag{3}$$

where τ is the relaxation time, G_0 is the plateau modulus, and ω is the angular frequency (rad s^{-1}), equal to $2\pi\nu$, where ν is the experimental oscillatory frequency (in s^{-1}). This relationship gives the relaxation time as the reciprocal of the angular frequency at the crossover of G' and G'',

$$\tau = \frac{1}{\omega} \text{ or } \tau = \frac{1}{2\pi\nu} \tag{4}$$

as well as G_0 from the high-frequency ($\omega^2\tau^2 \gg 1$, see eq 2) plateau in G'. Finally the zero-shear viscosity, η_0, is observed in the low-frequency limit as a plateau in the complex viscosity, $\eta^* = \sqrt{G'^2+G^2}/\omega$.[15] Any of these three parameters can be determined from the other two, according to

$$\eta_0 = G_0\tau \tag{5}$$

Thus G_0 may be obtained either by direct observation or from η_0 and τ by using eq 5. G_0 is directly proportional to the density of entanglement points in the system, and thus can be used to estimate the entanglement length, ξ, or average distance between these points, by[16]

$$G_0 \approx \frac{kT}{\xi^3} \tag{6}$$

Relaxation functions, $G(t)$, were determined by converting the dynamic ($G^*(\omega)$) data to a relaxation spectrum, using a computer program employing a nonlinear regularization[17] technique, as implemented by Phan-Thien et al.[18] Relaxation spectra were verified by calculating G' and G'' from the spectra, and comparing with the experimental data. $G(t)$ was then calculated according to[15]

$$G(t) = \int_{-\infty}^{\infty} He^{-t/\tau}\, \mathrm{d}\ln\tau \tag{7}$$

where H is the relaxation spectrum.

The overall (single) relaxation time can be considered a combination of characteristic times associated with relaxation of the aggregates by reptation (τ_{rep}), and their breaking time (τ_{br}). In the limit of fast breaking this is given by[19]

$$\tau = (\tau_{br}\cdot\tau_{rep})^{1/2} \tag{8}$$

When $\tau_{br} \ll \tau_{rep}$, The relaxation function, $G(t)$, decays as a single exponential given by

$$G(t) = G_0 \exp(-t/\tau) \tag{9}$$

When $\tau_{rep} \ll \tau_{br}$, the relaxation mechanism is effectively pure reptation. This gives a stretched exponential reflecting the polydispersity of the system[19]

$$G(t) = G_0 \exp[-(t/\tau)^{\alpha}] \tag{10}$$

where $\alpha = 0.25$ for a Gaussian distribution of chain lengths.

Dynamic data can be fitted to eq 10 by using values for G_0 determined as described above, and keeping α and τ as fitted parameters. The fitted value of α approaches unity in a Maxwellian system, as for eq 9. The more polydisperse the relaxation spectrum, the more α approaches the predicted exponent of 0.25 for polydisperse, permanent chains.

SANS experiments were performed on the NG-3 30m small angle neutron scattering spectrometer at the National Centre for Neutron Research at the National Institute of Standards and Technology, Gaithersburg, MD. The neutron beam had an average wavelength of $\lambda = 6$ Å ($\Delta\lambda/\lambda = 0.15$). Sample-to-detector distances of 1.40 and 13.1 m were used, accessing a range of scattering vectors (q, defined as $(4\pi/\lambda)\sin\theta$, where 2θ is the scattering angle) of $0.027 < q < 0.37$ Å^{-1}. Raw scattering data were corrected for detector background and sensitivity, and empty cell scattering. The resulting scattering functions were converted to absolute intensities by using precalibrated secondary standards provided by NIST. Finally, for each sample the incoherent background was determined from a plot of $I(q)\cdot q^4$ vs q^4 (ref 20) and found to be approximately 0.1 cm^{-1}. The incoherent backgrounds were subtracted over the whole q-range to give corrected absolute scattering functions.

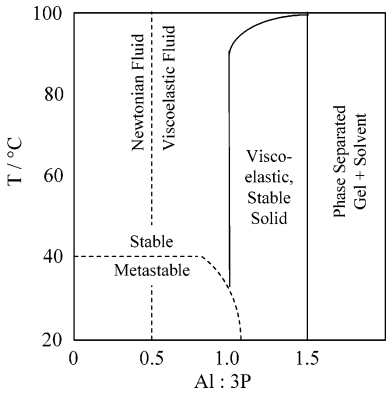

Figure 2. Schematic diagram of aluminum didodecyl phosphate organogel behavior at ~1% w/w surfactant, showing the effect of the Al:P ratio and temperature on dynamic behavior of the gels. Note that the boundaries shown are approximate, and depend on concentration.

Results

Figure 2 summarizes our observations of the behavior of aluminum didodecyl phosphate in decane as a function of the aluminum to phosphate surfactant ratio, Al:P. At low aluminum content (Al:P ≪ 1:3) the system behaves as a Newtonian fluid. As Al:P is increased, the system becomes increasingly viscoelastic. At ~1% w/w surfactant concentration, this occurs at Al:P of ~0.5:3. Between Al:P = 0.5:3 and 1.0:3, the gels are

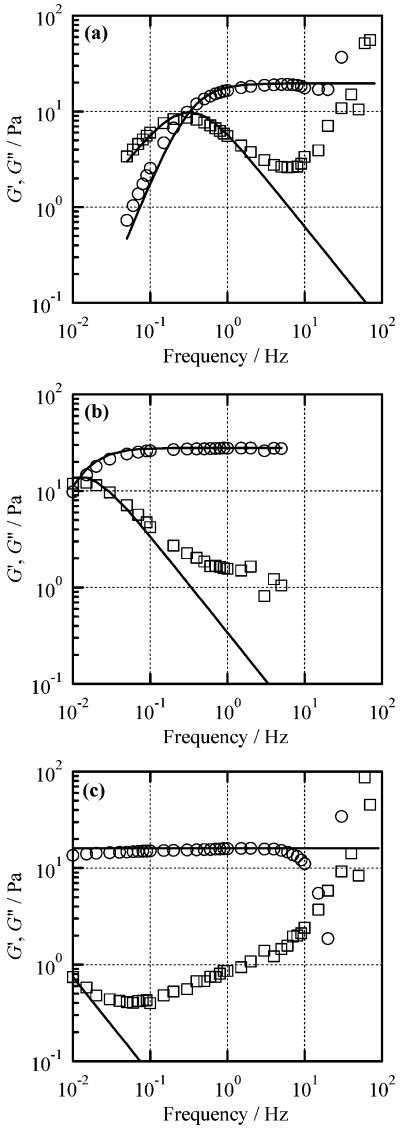

Figure 3. Dynamic oscillatory rheology of aluminum isopropoxide + didodecyl phosphate organogels ($\phi = 0.8\%$ w/w) at Al:P = (a) 1.0:3, (b) 1.06:3, (c) 1.2:3: ○, elastic modulus G'; □, loss modulus G''. Solid lines are single-relaxation Maxwell model fits to G' and G''.

viscoelastic fluids. They are also metastable at room temperature, separating over time into an opaque waxlike substance and Newtonian fluid. This eventual two-phase system reverts immediately to a single phase above ~40 °C. Above Al:P = 1.0:3, the gels change from fluidlike to a viscoelastic solid, which does not flow on experimentally accessible time scales. Finally, above around 1.5:3 a rapid, nonreversible phase separation occurs into a clear, isotropic gel and nonviscoelastic fluid. Qualitatively this progression with addition of aluminum is strikingly similar to that of lecithin organogels, where addition of water induces growth of wormlike aggregates, accompanied by increased viscosity and eventual phase separation.[21]

The approximate locations of the Al:P boundaries delineating these regions are also shown in Figure 2. However, precise specification of the respective transitions is concentration dependent. Within the viscoelastic gel region there are clearly significant changes in the rheological properties with changing Al:P ratio. Rheological studies were carried out over the range 0.5:3 to 1.5:3 to quantify this behavior.

Figure 3 shows dynamic oscillatory shear data for compositions of (a) 1.0:3, (b) 1.06:3, and (c) 1.2:3. These typify results for Al:P ratios across the transition from liquid to solid gel phase

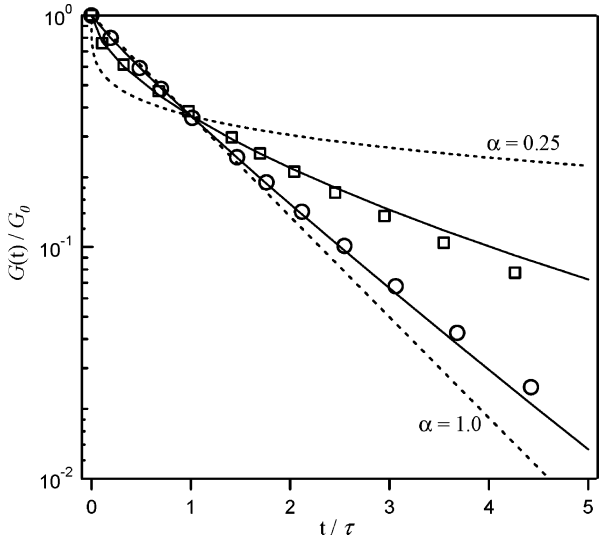

Figure 4. Normalized relaxation functions $G(t)/G_0$ vs normalized time t/τ: ○, Al:P = 1.00:3 (Figure 3a), $\alpha = 0.91$, $\tau = 0.36$ s; □, Al:P = 1.06:3 (Figure 3b), $\alpha = 0.60$, $\tau = 3.4$ s. Solid lines are the best fits of α and τ to eq 10, using experimental values for G_0, with as-fitted parameters. Dashed lines show the relaxation functions for the limiting cases $\alpha = 1.0$ ($\tau_{br} \ll \tau_{rep}$) and $\alpha = 0.25$ ($\tau_{rep} \ll \tau_{br}$).

(Figure 2). For Al:P ≤1.0:3 (Figure 3a), the data are Maxwellian with a single relaxation time, determined from the reciprocal of the crossover between G' and G'' (eqs 2−4). This behavior occurs for an entangled network of rodlike aggregates undergoing a reversible chain scission process,[19] as has been observed previously in both aqueous and nonaqueous self-assembled surfactant systems.[7,9,22,23]

As Al:P increases above 1.0:3, the data show increasing deviation from Maxwellian behavior (Figure 3b). The relaxation time increases (crossover frequency decreases) dramatically, and G'' departs from the expected $1/\omega$ behavior at lower frequency than entangled aggregates (Figure 3a). This behavior at low frequency is characteristic of a physical gel network.[24] For gels above about Al:P = 1.07:3 (e.g. Figure 3c), no crossover of G' and G'' occurred in the experimentally accessible frequency range, although a plateau in G' is clearly observed at all compositions. These gels are also thermally reversible, with a "melting" temperature of >90 °C.

Figure 4 shows normalized relaxation function of two representative samples in the viscoelastic gel region. For Maxwellian behavior, expected in the limit of fast breaking, $G(t)$ is a purely exponential function (eq 9), and the data approach this limit at Al:P = 1.0:3 with $\alpha = 0.91$. At a higher aluminum content of 1.06:3, the relaxation time is much longer, 3.4 s versus 0.36 s, and the relaxation function is more stretched (eq 10), with $\alpha = 0.60$. This clearly shows how the behavior changes from nearly exponential (Maxwellian) to highly stretched exponential with increasing aluminum content, indicative of a relaxation mechanism dominated by reptation of chains that are quite polydisperse in their lengths.

The change in the gel behavior is best illustrated by the relaxation time of the gel as a function of composition (Figure 5a). Between Al:P = 0.8:3 and 1.0:3, τ increases gradually. In this composition range the surfactant is in excess, so aggregate size is constrained by the available aluminum. The relaxation time increases with aggregate size, which increases τ_{rep}. However, as Figure 3a shows, an abrupt increase in relaxation time of *at least 3 orders of magnitude* occurs over a narrow composition range between Al:P = 1.0:3 and 1.1:3. The longest relaxation times shown here, i.e., those above about 50 s, were

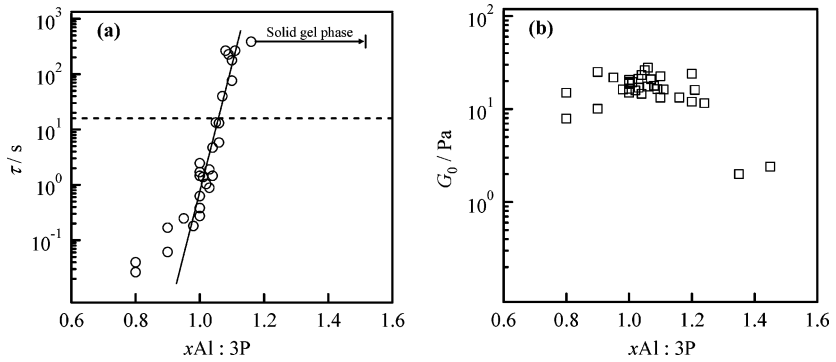

Figure 5. (a) Relaxation time, τ, and (b) Plateau modulus, G_0, as a function of Al:P ratio. The x-axis shows the molar quantity of aluminum, per 3 mol of phosphate in the system. The dashed line in part a shows the approximate upper limit of relaxation times experimentally observed by intersection of G' and G''. The solid line is a guide to the eye.

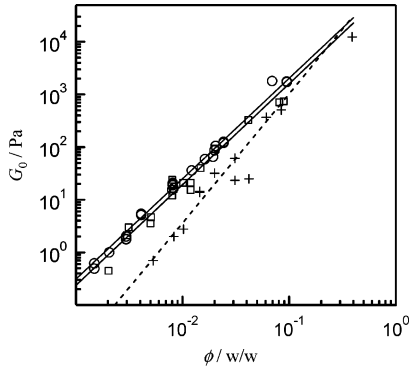

Figure 6. Scaling of the plateau modulus with gel volume fraction at various Al:P ratios: ○, 1.0:3; □, 1.2:3; +, 1.35:3. Solid lines show power law fits with exponents $n = 1.9$ at Al:P = 1.0:3 and 1.2:3 and $n = 2.5$ at Al:P = 1.35:3.

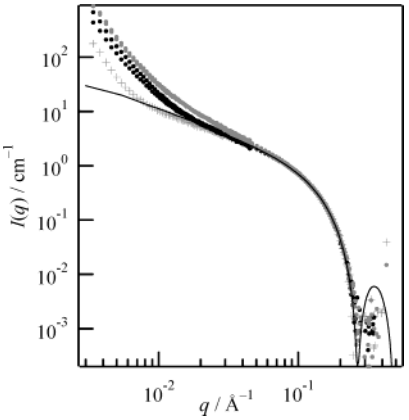

Figure 7. Small-angle neutron scattering curves of decane gels containing 2 wt % organogelator as a function of Al:P ratio: +, 0.5:3; dark solid circle, 0.8:3 and 1.0:3; gray solid circle, 1.1:3 and 1.2:3. The solid line is a fit to the high-q data of Al:P = 0.8:3, using a homogeneous, rigid rod model with an average fitted radius of 14.4 ± 0.2 Å.

estimated by extrapolation of single relaxation (Maxwell) fits to the storage and loss moduli (see e.g. Figure 3c). The actual size of this transition is probably even greater than shown, but we could not extrapolate fits to obtain very slow relaxation times with any degree of confidence above Al:P = 1.1:3.

G_0 remains unchanged over the range of this transition and to much higher aluminum content (Figure 5b), suggesting the absence of a fundamental change in the shape of the aggregates.

As described above (see Figure 2), gels below Al:P = 1.0:3 are metastable and separate over a few days into a waxlike solid and liquid. (This is somewhat dependent on the actual Al:P ratio, with stability increasing with increasing aluminum levels.) At aluminum levels above that of the step transition the gel is stable indefinitely (for several years). The onset of this long-term stability corresponds closely to the step transition in τ.

At the stoichiometric composition of Al:P = 1.0:3, the metastability at room temperature is reminiscent of the dihexadecyl phosphate/hexadecane system.[8] However, a reverse hexagonal phase was found by Fukasawa et al. at ~65 °C, which in this case was not detected either by differential scanning calorimetry or visual observation through crossed polarizers.

Increasing the aluminum content also significantly alters the rheology and stability of didodecyl phosphate/aluminum isopropoxide/decane organogels. We therefore expect the local aggregate structure found by Fukasawa et al. (Figure 1) to be modified by the presence of isopropoxyl moieties.

Figure 6 shows the scaling behavior of the plateau modulus with volume fraction of gelator at various Al:P ratios. Gels on both sides of the step transition scale as $G_0 \approx \phi^{1.9}$, which agrees with the exponent of 2−2.25 expected for entangled wormlike aggregates.[25] However, at Al:P = 1.35:3, the data are more scattered, and the fitted exponent of 2.5 is outside this predicted range. This composition is close to those where these gels macroscopically phase separate. We interpret these results, together with the decrease in G_0 (Figure 5b), as indicating microphase separation of the gel network before macroscopic separation is detected.

Figure 7 shows SANS spectra of 2.0% w/w organogelators with a range of Al:P ratios between 0.5:3 and 1.2:3. The spectra at all compositions are almost identical at high q, showing that the local structure of the aggregates is the same, but they differ at low q, indicating structural differences on longer length scales.

In the range $q > 0.05$ Å^{-1} the spectra are all well described by a model of homogeneous rigid rods with radii of 14.4 ± 0.2 Å (solid line, Figure 7). The scattered intensity also scales approximately as q^{-1} as expected for locally cylindrical structures. The locally cylindrical structure is clearly seen from the oscillations in a Porod plot ($q^4 \cdot I(q)$ vs q; Figure 8a). The slope of a "Guinier-like plot" ($\ln(q \cdot I(q))$ vs q^2; Figure 8b)[26,27] yields the radius of gyration of the cylinder cross-section ($R_{g,c}$), which is 11.3 ± 0.3 Å. This is in reasonable agreement with the fitted radius. In fact, if we assume a homogeneous scattering length density (SLD) of the cylinders, the radius corresponding to this radius of gyration is 16.0 ± 0.4 Å ($R_{g,c} = R/\sqrt{2}$). However, the quoted errors reflect only the scatter in the fitted values between Al:P ratios, not the absolute accuracy of the measurement. The discrepancy of 1.5 Å can be attributed to, for example, inhomogeneities in the scattering length density of the cylinders (i.e. penetration of solvent in the alkyl shell),

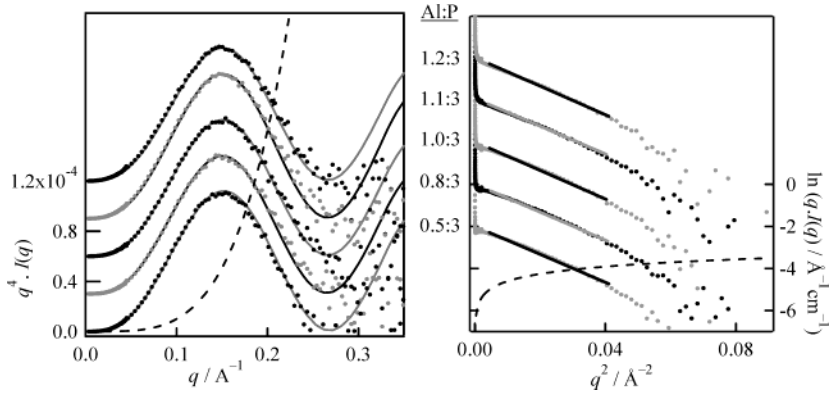

Figure 8. (a) Porod plots of gels at Al:P = 0.5−1.2:3, with fits over the range $0.5 < q < 0.3$; (b) Guinier-like plots of the same data, with linear least-squares fits over the range $0.005 < q^2 < 0.04$. The data for each of the compositions 0.8:3−1.2:3, which are otherwise indistinguishable from the 0.5:3 data, have been offset for clarity. The dashed lines show the intensity of incoherent background (with respect to Al:P = 0.5:3), which was previously subtracted from the raw data.

and the fact that the radius is near the limit of resolution of the measurement. The values are clearly independent of the Al:P ratio (Figure 8b), indicating that the local structure is unaltered across the composition range studied.

The fitted radius is smaller than the 21.6 Å expected from bond lengths and ionic radii for the core, and the empirical (all-trans) alkyl chain length[2] is due to the freedom of the tails to adopt other conformations and smearing of the contrast from solvent penetration between the alkyl tails. This structure is consistent with the proposed local structure (Figure 1) of molecularly thin rodlike aggregates, and is similar to that found by Terech et al.[9,23] for bicopper tetracarboxylate organogels, which have similar dynamic (rheological) behavior.

At low q the spectra begin to diverge from one another, all exhibiting a strong upturn in scattering below $q = 0.01$ Å^{-1}. This behavior can arise either from interference between multiple entangled aggregates, which are semidilute at 2% w/w concentration, i.e. structure factor effects, or to the presence of extended structures, i.e. form factor effects, which are only partially probed within the q-range of the experiment, and the two effects are difficult to distinguish by SANS.[28]

The plateau modulus yields an average entanglement length, ξ, of approximately 400 Å (eq 6), independent of Al:P up to 1.35. Although this is within the accessible q-range of these experiments, the SANS spectra exhibit no feature corresponding to this distance.[29] The increase in long-range structure with increasing Al:P is consistent with the formation of a network, and hence with both the rheology and the observation of macroscopic phase separation above Al:P = 1.5. This may arise from attractive interactions leading to adhesive contacts between aggregates, or from the formation of a branched network (see below).

The upturn extends to higher q with increasing aluminum content so that the intermediate q-range ($0.01 \le q \le 0.1$ Å^{-1}) spectra cluster in three groups: (i) Al:P = 0.5:3, which is well below the transition and where there is insufficient aluminum to complex all of the dodecyl phosphate, lowering the volume fraction of organogelator; (ii) compositions just below the gel transition, Al:P = 0.8:3 and 1.0:3; and (iii) compositions just above the transition, Al:P = 1.1:3 and 1.2:3. Above Al:P = 1.0:3 the aluminum is in excess, so the volume fraction of the organogelator aggregates is fixed.

The SANS spectra also show that $I(q)$ changes from a q^{-1} or rigid rod scaling behavior below the step transition to $\sim q^{-1.5}$ scaling above the transition with increasing Al:P, in the intermediate q range, $0.01 < q < 0.1$ Å^{-1}. The slope approaches the $q^{-5/3}$ behavior predicted[16] for excluded volume chains, and suggests that the aggregates may become more flexible as Al:P increases. (Because of the small q range exhibiting this behavior, this interpretation is somewhat speculative. The flexibility of wormlike aggregates can also be determined from small-angle scattering data by the use of a so-called Holtzer or bending-rod plot.[26,30] We attempted such an analysis of these data to substantiate these conclusions; however, the rapidly increasing scattered intensity at low q obscures any maxima in the relevant region.)

Discussion

Over a narrow composition range, Al:P = 1.0−1.1:3, these systems exhibit a 1000-fold jump in their structural relaxation time, accompanied by a transition from Maxwellian (living polymer) to non-Maxwellian (physical gel) rheology while maintaining a constant plateau modulus, and a change in the scattering behavior in the intermediate and low q range, while the local cylindrical structure is preserved. These coincide with the stoichiometry of the system changing from excess alkyl phosphate surfactant to excess aluminum.

The increase in relaxation time at the "step transition" (Figure 5) cannot be explained in terms of fast-breaking or living polymer systems, and in any case the relaxation spectrum indicates a change toward relaxation by pure reptation. A large increase in τ_{rep} is required to explain the large observed increase in the overall τ.

We infer from all this that the observed increase in relaxation time must be a result of connections between self-assembled rods, either in the form of branching or adhesion between the rods. Both of these mechanisms could lead to such a marked increase in relaxation time by the formation of long-lived or permanent connections between the aggregates.

Leibler et al.[31] have described how sticky contacts between polymer chains increase the relaxation time by slowing reptation, and that the modulus depends on the density of both entanglements and sticking points. Such interaggregate adhesion has been previously observed by Terech et al.[9] in bicopper tetracarboxylate organogels. In this case, however, the transition was induced by changing temperature rather than composition. The rheological effect was also far less pronounced than we observed here.

In the present system there is no obvious chemical mechanism that would lead to increasingly sticky interactions in excess aluminum isopropoxide. This suggests that the extended structure accompanying physical gel formation arises from the

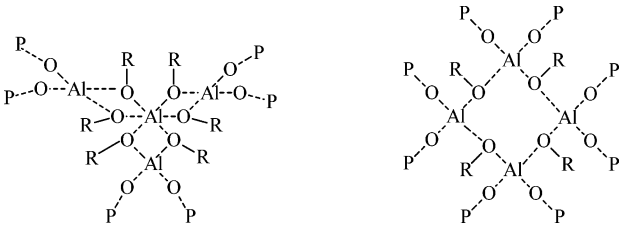

Figure 9. Oligomeric aluminum isopropoxide structures shown by Bradley et al.[34] (Figures 3.10 and 3.12), where R = isopropyl, $(CH_3)_2$-CH−. Sites at which isopropoxide (O−R) could be substituted by O−P bonds of alkyl phosphates are designated by O- -P. In these and other structures given in Bradley et al., aluminum can be 4-, 6-, or even 5-coordinated.

formation of a network of branched rods. The reptation of a branched chain with fixed or long-lived branch points is slowed exponentially compared with an unbranched chain.[16] Branching in self-assembled wormlike aggregates has been observed previously in lecithin water-in-oil microemulsions.[32,33] However, these dynamic branch points provide an additional stress relaxation mechanism due to the ability of a branch point to move in a "zipper-like" fashion along a chain and result in a decrease in relaxation time.

How can permanent or long-lived branches arise in the aluminum alkyl phosphate sytem? Increasing Al:P above the stoichiometric ratio of 1:3 results in a fraction of undisplaced isopropoxide remaining coordinated to aluminum incorporated into the self-assembled aggregates. This is the only significant difference between this in situ gel formulation and the dispersed aluminum dialkyl phosphate system.[8] Aluminum isopropoxide itself is known to exist as dimers, trimers, and tetramers, examples of which are shown in Figure 9, in which isopropoxide can act as a bridging ligand.[34] We therefore expect that it can remain similarly coordinated to the aluminum in place of dialkyl phosphate groups. Furthermore, if substituted by aluminum−surfactant aggregates in three or more directions, these naturally occurring oligomers allow the formation of various chemical branch points connecting the aggregates; the oligomers shown in Figure 9 would yield 3- and 4-armed branches, respectively. There need only be a small number of these fixed branch points to have an enormous effect on τ_{rep},[16] consistent with the steepness of the step transition.

If this is the case, then the number of these branch points should increase as the excess of aluminum is increased. Given a constant overall aggregate concentration, these branch points replace entanglements, leaving the overall value of G_0 constant, since the total density of (branches + entanglements) cannot change without a phase separation or a significant change in aggregate structure, but increasing relaxation time.

As the excess of aluminum is further increased, the relative contribution to G_0 of physical branch points approaches 1, and phase separation will occur into a saturated gel with excess solvent excluded,[35,36] as we observe experimentally (Figure 2).

The change in stability of the gels across the transition (in the one-phase region) can also be explained by the formation of connection points in the system. The presence of a significant number of these points allows us to consider the system as an infinite network of interconnected aggregates, as opposed to a network of transient independent aggregates. In the same way that they prevent reptation, branches would prevent the aggregates from flocculating by maintaining a physical separation related to the finite flexibility of the chains. Such a system will occupy some natural volume.[16,35] If this is greater than the volume of solvent available (determined by the concentration of the solution), then the force between branch points is necessarily repulsive. As the aluminum excess increases, the branch point density will also increase, compacting the network and forcing out excess solvent,[33] resulting in the observed phase separation.

This mechanism provides an explanation for the drop in the plateau modulus (Figure 5) observed close to the phase separation, and the accompanying change in the scaling behavior. As G_0 is constant as a function of Al:P before the onset of separation, a drop in G_0 can then be considered an indication of the phase separation on a microscopic scale: An alternative relaxation mode becomes available, in the form of movement between the microscopic gel-phase regions which become separated by regions of the second, nonelastic phase. This lowers G_0 by masking the elastic response of the connections within the gel phase, as is observed for example at the onset of phase separation in surfactant lamellar phases.[37]

Furthermore, assuming the equilibrium volume occupied by the connected network at a given Al:P is independent of concentration, the phase limit must shift with concentration. Thus at constant Al:P of 1.35:3, for example (see Figure 6), the degree of phase separation (i.e. the proportion of excluded solvent) will decrease with increasing concentration, so the G_0 value approaches that of the unseparated samples (1.0 and 1.2:3 in Figure 6). This would explain the altered scaling behavior of the plateau modulus at 1.35:3 as an artifact of a microscopically phase-separated system. In this case at ~10% w/w, as a rough approximation, the system would be at the phase limit at Al:P = 1.35:3.

Conclusions

Mixtures of aluminum isopropoxide and didodecyl phosphoric acid in decane form self-assembled organogels consisting of locally cylindrical aggregates whose structure and properties depend sensitively on the presence of excess aluminum. With excess surfactant, an entangled network of aggregates exhibits Maxwellian rheology reminiscent of wormlike micellar systems or reversibly cross-linked polymers. However, an excess of aluminum isopropoxide facilitates the formation of interaggregate connections that dramatically increase the relaxation time of the gel, corresponding to a transition from independent wormlike aggregates to a physical gel network. At large excess of aluminum this ultimately leads to solvent exclusion in the form of phase separation between gel and excess solvent.

The changes in behavior with excess aluminum can be explained by the formation of long-lived branch points in the aggregates that slow relaxation by hindering reptation. We suggest that such branches may form from naturally occurring aluminum isopropoxide oligomers. Additional data are required to determine precisely the effect of the excess aluminum isopropoxide on the accompanying structural modification suggested by the small angle scattering data.

Acknowledgment. We acknowledge funding from the Australian Research Council SPIRT scheme, the Australian Nuclear Science and Technology Organisation, and Rhodia Inc., as well as the support of the Rheology Group at the Department of Mechanical Engineering, University of Sydney, in providing facilities used in this work. This work utilized facilities supported in part by the National Science Foundation under Agreement No. DMR-9986442. We acknowledge the support of the National Institute of Standards and Technology, U.S. Department of Commerce, in providing the neutron research facilities used in this work.

References and Notes

(1) Terech, P. Low-Molecular Weight Organogelators. In *Specialist Surfactants*; Robb, I. D., Ed.; Chapman & Hall: New York, 1997; p 208.

(2) Tanford, C. *The Hydrophobic Effect*: *Formation of Micelles and Biological Membranes*, 2nd ed.; Wiley: New York, 1980.

(3) Eicke, H. F. Surfactants in Nonpolar Solvents. In *Topics in Current Chemistry*; Boshke, F. L., Ed.; Springer-Verlag: Berlin, Germany, 1980; Vol. 87, p 85.

(4) Hoffmann, H.; Ulbricht, W. *Curr. Opin. Colloid Interface Sci.* **1996**, *1*, 726.

(5) Tachibana, T.; Mori, T.; Hori, K. *Bull. Chem. Soc. Jpn.* **1980**, *53*, 1714.

(6) Terech, P. *Colloid Polym. Sci.* **1991**, *269*, 490.

(7) Shchipunov, Y. A. *Colloids Surf., A* **2001**, *183*, 541.

(8) Fukasawa, J.-I.; Tsutsumi, H. *J. Colloid Interface Sci.* **1991**, *143*, 69.

(9) Dammer, C.; Maldivi, P.; Terech, P.; Guenet, J. M. *Langmuir* **1995**, *11*, 1500.

(10) Monroe, R. F.; Rooker, B. E. Aluminum dialkyl phosphates lubricant additives, U.S. Patent 3,494,949, 1970.

(11) Rose, S. H.; Block, B. P. *J. Am. Chem. Soc.* **1965**, *87*, 2076.

(12) Crescenzi, V.; Giancotti, V.; Ripamonti, A. *J. Am. Chem. Soc.* **1965**, *87*, 391.

(13) Huddleston, D. A. *Liquid Aluminium Phosphate Salt Gelling Agent*; U.S. Patent 5,202,035, 1993.

(14) Kim, V.; Bazhenov, A. V.; Kienskaya, K. I. *Colloid J.* **1997**, *59*, 455.

(15) Ferry, J. D. *Viscoelastic Properties of Polymers*, 3rd ed.; Wiley: New York, 1980.

(16) De Gennes, P.-G. *Scaling Concepts in Polymer Physics*; Cornell University Press: New York, 1979.

(17) Honerkamp, J.; Weese, J. *Rheol. Acta* **1993**, *32*, 65.

(18) Phan-Thien, N.; Safari-Ardi, M. *J. Non-Newtonian Fluid Mech.* **1998**, *74*, 137.

(19) Cates, M. E. *Macromolecules* **1987**, *20*, 2289.

(20) *Neutron, X-Ray and Light Scattering*: *Introduction to an Investigative Tool for Colloidal and Polymeric Systems*; Lindner, P., Zemb, T. N., Eds.; North-Holland: Amsterdam, The Netherlands, 1991.

(21) Shchipunov, Y. A.; Schmiedel, P. *Langmuir* **1996**, *12*, 6443.

(22) Shikata, T.; Hirata, H.; Kotaka, T. *Langmuir* **1987**, *3*, 1081.

(23) Terech, P.; Maldivi, P.; Dammer, C. *J. Phys. II* **1994**, *4*, 1799.

(24) Ross-Murphy, S. B. *Ber. Bunsen-Ges.* **1998**, *102*, 1534.

(25) In, M.; Warr, G. G.; Zana, R. *Phys. Rev. Lett.* **1999**, *83*, 2278.

(26) Magid, L. J.; Li, Z.; Butler, P. D. *Langmuir* **2000**, *16*, 10028.

(27) Lin, T.-L.; Chen, S.-H.; Gabriel, N. E.; Roberts, M. F. *J. Phys. Chem.* **1987**, *91*, 406.

(28) Lum Wan, J. A.; Warr, G. G.; White, L. R.; Grieser, F. *Colloid Polym. Sci.* **1988**, *265*, 528.

(29) Warr, G. G.; Magid, L. J.; Caponetti, E.; Martin, C. A. *Langmuir* **1988**, *4*, 813.

(30) Schmidt, M.; Paradossi, G.; Burchard, W. *Makromol. Chem., Rapid Commun.* **1985**, *6*, 767.

(31) Leibler, L.; Rubinstein, M.; Colby, R. H. *Macromolecules* **1991**, *24*, 4701.

(32) Shchipunov, Y. A.; Hoffmann, H. *Langmuir* **1998**, *14*, 6350.

(33) Cirkel, P. A.; Vanderploeg, J. P. M.; Koper, G. J. M. *Phys. Rev. E* **1998**, *57*, 6875.

(34) Bradley, D. C.; Mehrotra, R. C.; Gaur, D. P. *Metal Alkoxides*; Academic Press: London, UK, 1978.

(35) Flory, P. *Principles of Polymer Chemistry*; Cornell University Press: New York, 1971.

(36) Drye, T. J.; Cates, M. E. *J. Chem. Phys.* **1992**, *96*, 1367.

(37) Petrov, P. G.; Ahir, S. V.; Terentjev, E. M. *Langmuir* **2002**, *18*, 9133.